Biosensors and Bioelectronics 25 (2009) 362–367

Contents lists available at ScienceDirect

Biosensors and Bioelectronics

journal homepage: www.elsevier.com/locate/bios

A cuttlebone-derived matrix substrate for hydrogen peroxide/glucose detection

Guilan Xu, Hui Li, Xiaoyuan Ma, Xueping Jia, Jian Dong, Weiping Qian*

State Key Laboratory of Bioelectronics, School of Biological Science and Medical Engineering, Southeast University, Nanjing 210096, PR China

ARTICLE INFO

Article history:
Received 30 April 2009
Received in revised form 17 July 2009
Accepted 17 July 2009
Available online 25 July 2009

Keywords:
Biosensors
Cuttlebone-derived matrix substrate
Gold nanoparticles
Glucose
LSPR

ABSTRACT

A simple biosensor for hydrogen peroxide (H_2O_2) and glucose was fabricated by incorporating gold nanoparticles (GNPs) onto a cuttlebone-derived matrix substrate (CDMS). Such a three-dimensional chamber-like structure naturally bears abundant amino groups for the direct immobilization of GNPs without a series of modifications. And preferably, the framework endows CDMS with a very high surface area for the attachment of GNPs, resulting in effective optical signal transduction and improved sensitivity of the detection system. The principle behind this biosensor is that the localized surface plasmon resonance (LSPR) of the immobilized GNPs changes with the enlargement of GNPs by H_2O_2-mediated chemical reduction of chloroauric acid. Using this approach, we demonstrate the proof of an optical biosensor to quantify the concentration of H_2O_2 as well as glucose. UV–vis absorption spectra were recorded to obtain quantitative information about the H_2O_2 or glucose concentration. The detection range of our biosensor to H_2O_2 concentration was from 2×10^{-6} to 1.5×10^{-4} M, while the linear response range of glucose concentration was from 5×10^{-6} to 5×10^{-5} M. Inspiringly and interestingly, the growth of GNPs on CDMS gives rise to color changes, this phenomenon shows that the rapid detection by our sensor has the superiority in visual detection to a certian extent, which has been a potential application in qualitative or semiquantitative analysis for medicine and biotechnology.

1. Introduction

Gold nanoparticles (GNPs) have attracted extensive interest because of their unique electronic, optical, and catalytic properties. The integration of GNPs into suitable matrixes is particularly useful for various applications, such as electrochemical sensors (Yu et al., 2003; Zhang et al., 2005; Zhou et al., 2006; Yang et al., 2007) and optical sensors (Xue et al., 2006; Shen et al., 2007; Zhang et al., 2007; Wang et al., 2007a,b). GNPs are so attractive due to their unique localized surface plasmon resonance (LSPR), which can be modulated by the size, the interparticle distance as well as the refractive index of the surrounding medium. Under the isolated approximation, their relationship can be expressed by Eq. (1) (Schmitt et al., 1999), where κ is the absorption coefficient, N is the numerical density of the nanoparticles, R is the radius of spherical particles, ε_1 and ε_2 are the real and imaginary parts of the dielectric constants of nanoparticles, and ε_m is the dielectric constant of the surrounding medium. Considering Eq. (1), the radius of spherical particle R is three cubed to the absorption coefficient κ, thus, sensors based on dimension change of GNPs have their sensitive superiority to others. This is the key challenge to biosensor design when transforming the bio-events or detection information into physically detectable signals. Although there have been efficient biosensors designed based on refractive index changes (Chen et al., 2005; Gu et al., 2002), such as antigen–antibody recognition, novel biosensors based on size-dependent amplitude change of absorption have emerged, especially in quantitative optical detection with their improved sensitivity (Shlyahovsky et al., 2005; Zayats et al., 2005; Baron et al., 2005).

$$\kappa = 6\pi N R^3 \frac{\varepsilon_m^{3/2}\varepsilon_2}{(\varepsilon_1 + 2\varepsilon_m)^2 + \varepsilon_2^2} \quad (1)$$

Some correlative work has been performed in solutions or on glass substrates (Zayats et al., 2005; Baron et al., 2005; Ma and Sui, 2002). However, an interesting application of cuttlebone-derived matrix substrates (CDMSs) instead of normal substrates has hitherto not received any attention. This could lead to a new class of smart composites that combine the beneficial features of CDMSs with those of the GNPs. The CDMSs, which were isolated from cuttlebones, have the strong complexation abilities of the amino groups (Ogasawara et al., 2000) with GNPs without additional introduction (Baron et al., 2005; Ding et al., 2006; Tan et al., 2006; Nath and Chilkoti, 2002). Moreover, their chamber-like framework gives the substrate a very high attachment capacity of GNPs, resulting in effectively optical signal amplification. Finally, cuttlebones are abundant in nature commonly known as seafood offal and can be obtained easily. Glucose detection is very importante in many practical areas such as food and fermentation analysis,

* Corresponding author. Tel.: +86 25 83795719; fax: +86 25 83795719.
E-mail address: wqian@seu.edu.cn (W. Qian).

0956-5663/$ – see front matter © 2009 Elsevier B.V. All rights reserved.
doi:10.1016/j.bios.2009.07.014

textile industry, environmental monitoring, and medical diagnosis, etc. A considerable amount of relevant methods for this purpose have been reported, including surface plasmon resonance biosensor, near-infrared optical biosensor, capacitive detection, electrochemiluminescene, fluorescence detection, colorimetry, and amperometric biosensor, etc. Much effort has been focused on developing suitable techniques for precisely monitoring the glucose level with high sensitivity, high reliability, fast response, good selectivity, and low cost (Wang et al., 2009; Yan et al., 2008; Wang et al., 2007a,b). In this paper, we represent an alternative route to design a biosensor for hydrogen peroxide (H_2O_2) and glucose detection by combining the GNPs with CDMSs. The substrate serves as a vehicle while the LSPR peak of the immobilized GNPs can be utilized for signal transduction. Direct use of the gold-functionalized CDMS as a size-dependent biosensor for optical quantitative detection for H_2O_2 and glucose was amply demonstrated. Simultaneously, the color changes of resulting modified substrates, from rose pink to mulberry, could be distinguished by the naked eye, which makes the biosensor a promising candidate for visual detection to a certian extent. Our basic process combined the first adsorption of small GNPs (3–5 nm) as gold seeds onto CDMSs and their further H_2O_2-mediated growth by deposition of gold on the seed faces. The gold seeds act as catalysts for the reduction of chloroauric acid by H_2O_2, resulting in enhanced absorbance features, Eq. (2) (Zayats et al., 2005).

$$AuCl_4^- + 3/2H_2O_2 \xrightarrow{\text{Gold seeds}} Au^0 + 4Cl^- + 3H^+ + 3/2O_2 \quad (2)$$

2. Experimental

2.1. Materials and equipment

All the cuttlebones were of Sepiella maindroni. Hydrogen tetrachloroaurate (III) hydrate ($HAuCl_4{\cdot}4H_2O$), sodium borohydride ($NaBH_4$), potassium carbonate (K_2CO_3), hydrogen peroxide, glucose were all purchased from Nanjing Sunshine Biotechnology Ltd., China. Glucose-oxidase (GOx, 100 units/mg) was purchased from Sigma. All reagents were used as received.

2.2. Fabrication of CDMSs

The lamellar part of a cuttlebone was cut into several pieces vertical to its natural lamella direction (size: 1 cm × 3 cm), and then soaked in 250 mL of 2 M HCl for 4 h under low vacuum. A low vacuum was used to exclude CO_2 bubbles, which formed during dissolution of the aragonite component, from the internal chambers of the organic matrix. This procedure was repeated several times in freshly prepared 2 M HCl until no bubbles came into being. The obtained organic matrixes were thoroughly washed with abundant distilled water for several times. During these processes, the lamellae of organic matrix eventually tended to be dissociative from each other, resulting in numbers of thin substrates. Afterwards, adding these semitransparent substrates to 250 mL of 0.5 M NaOH at a boiling temperature for 0.5 h to remove associated proteins. Such a treatment makes the substrates transparent and better for UV–vis characterization. Finally, these transparent substrates were also extensively washed with distilled water and stored at 4 °C before use. The stability of CDMSs is remarkable if they are kept at 4 °C, in this case, they can be normally stored at least longer than two months for low temperature. Several pieces of substrates were freeze-dried to do SEM analysis for the gentle removal of water.

2.3. Synthesis of GNPs

GNPs (3–5 nm) were prepared by the reduction of chloroauric acid with sodium borohydride according to literature procedures by our previous work (Ding et al., 2006). Typically, 3 mL of 1% $HAuCl_4$ solution was mixed with 200 mL of triply distilled water under vigorous stirring, followed by the addition of 1 mL of an aqueous solution of K_2CO_3 (0.2 M). Afterwards, 9 mL of $NaBH_4$ (0.5 mg/mL) solution was quickly added to the mixture. The final wine-red solution was stored at 4 °C until use. The concentration of the GNPs solution was calculated to be $\sim 2 \times 10^{14}$ particles/mL (Tan et al., 2006).

2.4. Immobilization of GNPs on CDMSs

The immobilization of GNPs on CDMSs was carried out as follows. Firstly, the CDMSs were soaked in the prepared GNPs solution. As a detail, every 10 pieces of substrates were immersed in 200 mL of GNPs solution at 4 °C for 3 h. The GNPs gradually attached to the surface of CDMSs due to the strong complexation abilities of the amino groups with GNPs (Bassi et al., 2000; Domard, 1987). Besides, the small size of the GNPs facilitated the gold seeds to access the huge interstitial space of the substrate and then attach to the surfaces. Finally, the gold-functionalized CDMSs were rinsed for at least three times to remove the unattached GNPs and kept in distilled water for later use. According to optical properties of gold-functionalized CDMSs during 1 week, the stability of gold-functionalized CDMSs which are kept in distilled water at 4 °C is identifiable for several days.

2.5. The quantitative detection for H_2O_2/glucose

A Shimadzu UV3150 UV–vis spectrophotometer (Japan) was used to measure the absorbance of immobilized GNPs on the surfaces of CDMSs. All samples were positioned in the standard glass cell with a home-made rectangular glass chip. The phosphate buffer solution of chloroauric acid was aged in refrigerator at 4 °C for 24 h before use. The process of H_2O_2 detection was depicted as follows. The gold-functionalized CDMS was first placed into a phosphate buffer solution (pH 7.4, 0.02 M) which contained the aged auric salts (1×10^{-4} M) and then variable concentration of H_2O_2 was added. The experiments were performed under vigorous shaking for 10 min at room temperature. During this step, the preadsorbed GNPs served as nucleation sites for electroless metal deposition. After rinsing thoroughly with distilled water, the UV–vis absorption spectrum of the resulting modified substrate in water was recorded over the range of 400–850 nm.

The analysis of glucose was also carried out using the gold-functionalized CDMSs which was similar to H_2O_2. Each gold-functionalized CDMS was interacted with 1×10^{-4} M $HAuCl_4$, 12 μg/mL GOx in the presence of glucose in 0.02 M phosphate buffer for 20 min at 32 ± 1 °C. The spectral changes of the resulting modified substrates in the presence of glucose with variable concentrations were also estimated by UV–vis spectrophotometer. Control experiments were performed in the absence of H_2O_2 or glucose.

3. Results and discussion

3.1. The structure of cuttlebone and CDMS films

Typically, an intact cuttlebone consists of a thin, hard, calcified, dorsal shield and a ventral porous phragmocene comprised of numerous narrow chambers, delineated by chitinous septa (Bandel and Boletzky, 1979). Such a shell, besides its skeletal structure, also functions as a rigid buoyancy tank that enables the cuttlefish to withstand external pressures and maintain a fixed position under seawater (Ogasawara et al., 2000; Jia et al., 2008; Jia and Qian, 2008; Jia et al., 2009). Fig. 1a shows the dorsal view of a whole cuttlebone cut through cross-section with its schematic map illustrated in Fig. 1b. The dorsal shield is a tough cover which overlays the lamellar matrix and seals off the separate chambers. The strategy

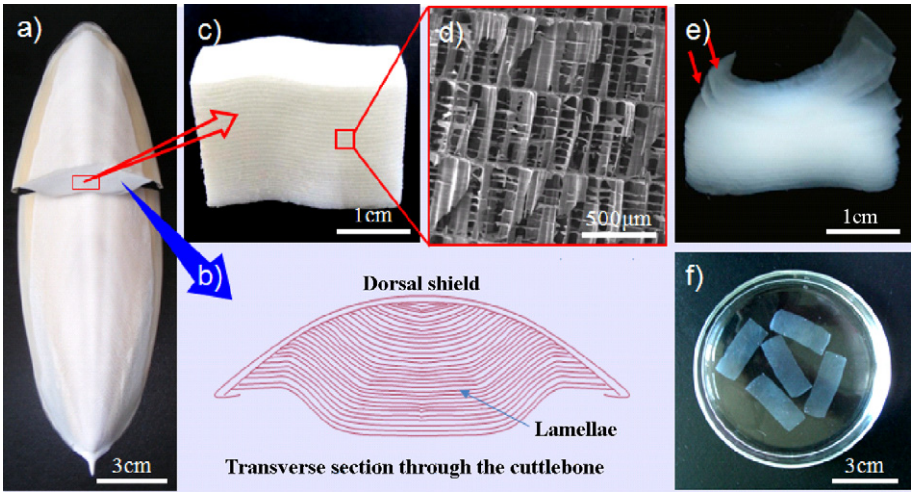

Fig. 1. Classical steps involved in the fabrication of CDMSs: (a) digital photograph of a dorsal-view cuttlebone cut though the cross-section and (b) schematically transverse section through the cuttlebone; (c) digital photograph of a block cut from lamellar part of the bone; (d) SEM image showing the chamber-like architecture of the area marked in (c); (e) digital photograph of cuttlebone-derived matrix after decalcification (two red arrows indicate the detached lamella, respectively); (f) digital photograph of several detached substrates presented in anaquarium dish.

for the fabrication of CDMSs involves several steps as follows. The lamellar part of the bone was used (red rectangle in Fig. 1a) and a typical one is shown in Fig. 1c. The lamellae grow naturally with a slight undulation and the well-organized lamellar structure can be seen clearly even with the naked eye. According to its SEM image in Fig. 1d, the bone has a chamber-like architecture in the form of mineralized sheets arranged in parallel layers and separated by sigmoidal pillars mentioned in our other correlative work. The spacing of each individual lamella varies in different areas of the bone but is usually between 200 and 600 μm (Birchall and Thomas, 1983). The distance between neighbouring pillars is ~100 μm and the interval space of each lamella is furthermore separated into small spaces by parallel sheets which are likely to provide an additional reinforcement to the bone. The demineralization of cuttlebone was carried out according to previous work with some modifications (Ogasawara et al., 2000; Jia et al., 2008; Jia and Qian, 2008; Jia et al., 2009). The obtained organic matrixes tended to be detached into individual ones along its naturally lamellar direction, two of which were indicated by red arrows as shown in Fig. 1e. Herein and in the following text, a substrate refers to each detached lamella of decalcified cuttlebone. Several detached lamellae were displayed in Fig. 1f. Within our biosensor fabrication, these lamellae were used as the optically transparent substrates for GNPs immobilization.

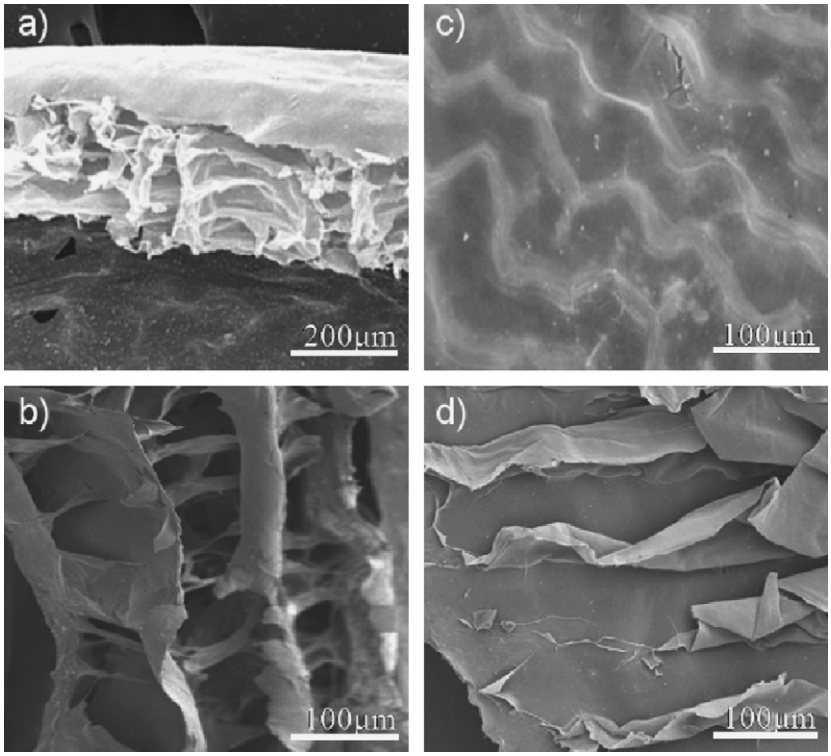

Fig. 2. SEM images showing the microstructure of CDMSs: (a) a piece of CDMS; (b) cross-sectional and (c) top-view images of a CDMS; (d) the pillars inside a CDMS with top sheets removed.

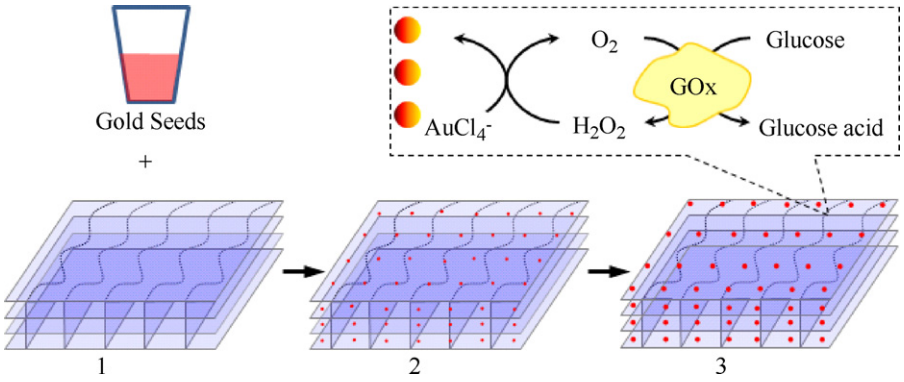

Scheme 1. Schematic illustration of the fabrication of gold-functionalized CDMS and its optical biosensing principle based on the biocatalytic GNPs growth in the presence of glucose. (1) Transparent CDMS, (2) functionalization of CDMS with gold seeds, (3) H_2O_2-mediated enlargement of GNPs on sensor for detection.

Such a decalcification process made it possible to isolate the organic matrix from rigid cuttlebone. Before GNPs immobilization, we first examined the morphology and microstructure of CDMSs. We found that the organic substrate was structurally continuous and retained the three-dimensional chamber-like architecture of the native biomineral observed prior to decalcification (Fig. 2a–d). Although the organic samples collapsed to some extent in the vacuum of the SEM, the chamber-like structure could be readily observed both in Fig. 2a and b. Fig. 2a shows the partial morphology of an isolated lamella. The lamella was supported both by organic wall structure and interconnected sheets which spanned and divided the interlayer space into air-filled chambers, ~100 μm × ~50 μm in size (Fig. 2b). Top-view analyses of the individual lamella reveal that the pillars in framework architecture were still arranged in an "S" fashion (Fig. 2c). The pillars inside the CDMS could be seen when top sheets were removed. Both the sheets and interlamellar pillars were continuous and smooth in texture.

The principle underlying our sensor and its fabrication is illustrated in Scheme 1. Exploiting the strong complexation abilities of the amino groups with GNPs (Bassi et al., 2000; Domard, 1987), CDMSs functionalization was achieved by one-step incubation of the isolated lamelae in GNPs solution. The H_2O_2-mediated enlargement of GNPs on the sensor is transduced to an enhanced optical signal which can be recorded by UV–vis spectrophotometer.

3.2. Optical properties of gold-functionalized CDMS films

To check the optical properties of gold-functionalized CDMSs, they were characterized by UV–vis spectrophotometer. Fig. 3a shows the UV–vis absorption spectrum of a substrate after adsorption of GNPs. An absorption peak at 520 nm can be observed. This peak can be assigned to the LSPR of the GNPs, indicating that nanosized gold particles were immobilized onto the surfaces of CDMSs. For comparison, the spectrum of the GNPs solution located at 510 nm is also shown in Fig. 3a. The aggregation of GNPs on a substrate or the formation of multilayers would result in the coupling of plasmons of individual particles and would be reflected in the UV–vis spectrum as an increased absorbance at wavelengths greater than 600 nm (Grabar et al., 1995). The absence of such a feature in Fig. 3a indicates that the GNPs are immobilized in a monolayer on the surfaces of CDMSs and are isolated from each other. Fig. 3b shows the adsorption dynamics of GNPs onto the CDMS surfaces at 4 °C in 24 h. This result shows that the adsorption kinetics of GNPs to CDMSs is directly related to the incubation time. By adjusting adsorption time, the amount of GNPs that were immobilized onto the substrates can be effectively modulated over a large range. Since the sensitivity of biosensor has a relationship with the number of attached GNPs from Eq. (1), it is also a novel strategy to amplify the detection signal by using CDMSs with high surface area and strong complexation abilities.

3.3. Biosensing for H_2O_2

Such gold-functionalized CDMSs were first used as a sensor for the direct detection of H_2O_2. As GNPs have a rich plasmon band, which is a function of their size and shape, the variations in GNPs dimension as well as the increased content of gold will surely lead to a change in their plasmon band. Thus, based on the H_2O_2-mediated

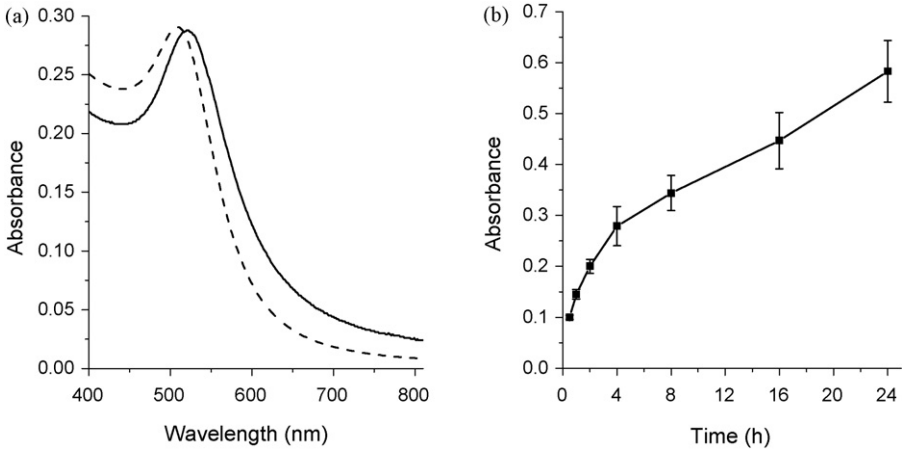

Fig. 3. (a) Absorbance spectrum of the gold-functionalized CDMS (solid line) and that of gold suspension (dashed line). (b) The adsorption dynamics of GNPs onto CDMSs as a function of time.

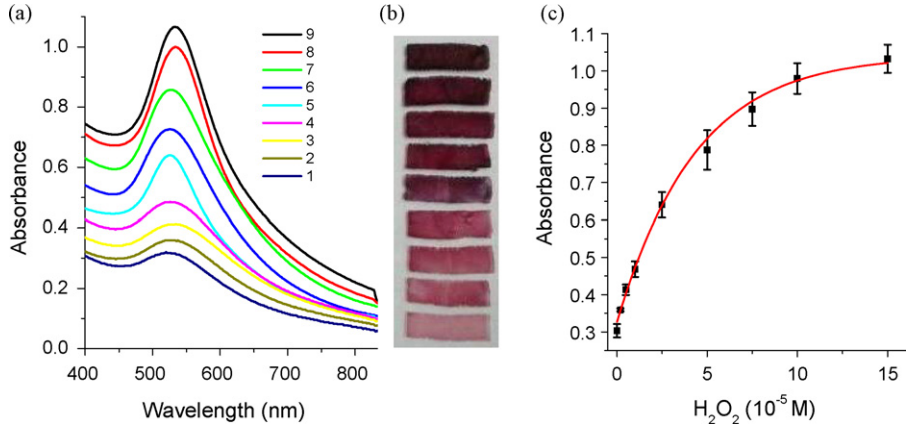

Fig. 4. (a) Absorbance spectra of the gold-functionalized CDMSs upon reaction with 1×10^{-4} M $HAuCl_4$ in phosphate buffer (pH 7.4, 0.02 M) that includes H_2O_2 of different concentrations at room temperature: (1) 0 M, (2) 2×10^{-6} M, (3) 5×10^{-6} M, (4) 1×10^{-5} M, (5) 2.5×10^{-5} M, (6) 5×10^{-5} M, (7) 7.5×10^{-5} M, (8) 1×10^{-4} M, (9) 1.5×10^{-4} M. (b) A digital photograph showing the differences in color of resulting modified substrates corresponding to the absorbance spectra 1–9, from the bottom up. (c) Calibration curve corresponding to the absorbance at $\lambda = 530$ nm of the gold-functionalized CDMSs upon analyzing H_2O_2 of variable concentrations (experimental conditions as in Fig. 4a). Error bars are the standards of three replicates.

growth of GNPs, the relationship between the spectral amplitude change and H_2O_2 concentration can be ultimately built for optical quantitative detection application. The series of UV–vis absorbance spectra in Fig. 4a clearly exhibit the evolution of optical absorbance of the resulting modified substrates in the presence of variable concentrations of H_2O_2. As the concentration of H_2O_2 increases, the reduction processes go forward and there are obvious enhancements in spectral intensity which indicate the growth of gold seeds on the CDMSs that yield the high absorbance features. Apart from their great amplitude change of absorbance spectra, the absorbance bands characteristic to the GNPs are constantly red shifted as the concentration of H_2O_2 is elevated. This phenomenon is reasonable and supports the H_2O_2-mediated GNPs growth mechanism discussed by the literature (Zayats et al., 2005). The resulting modified substrates, after reaction with increased concentration of H_2O_2, show significant color changes, from light pink to rosiness then mulberry, which could be discriminated by naked eye (Fig. 4b). Although, as the concentration of H_2O_2 increased to 10^{-4} M or more, their color changes were too deep to distinguish their differences. The color changes in substrates may be ascribed to the change of GNPs dimension and their spatial arrangements on the surfaces of CDMSs. This phenomenon encouraged us for its possible visual detection. The calibration curve corresponding to the optical detection of H_2O_2 is shown in Fig. 4c with a sensitivity limit that corresponds to 2×10^{-6} M. At low H_2O_2 concentration, the curve shows fine linearity. While H_2O_2 concentration increases to 5×10^{-5} M, the curve goes up slowly, but we still found that their absorbance change has its orderliness. The detection range of our biosensor to H_2O_2 concentration was from 2×10^{-6} to 1.5×10^{-4} M while the spectral intensity change was from ~0.3 to ~1.0. This response amplitude of spectral intensity was great higher than that from ~0.16 to ~0.26 with H_2O_2 concentration from 2×10^{-5} to 7.2×10^{-3} M on glass supports (Zayats et al., 2005). Furthermore, our detection limit of 2×10^{-6} M is also lowers than that of 2×10^{-5} M. This may due to the large amount of gold seeds immobilized on CDMS which can effectively catalyze the reduction of more $HAuCl_4$ by H_2O_2. According to the Eq. (1), the LSPR absorption mainly depends on the size of spherical particle rather than the dielectric constant of the surrounding medium. Besides, the amount of gold seeds also plays an important role in sensor sensitivity which can be related to the numerical density of the nanoparticles *N*. Inspiringly, different from their observation (Zayats et al., 2005), as the H_2O_2 concentration even increases to 10^{-4} M, no obviously small flakes separated from the parent GNP cores in the

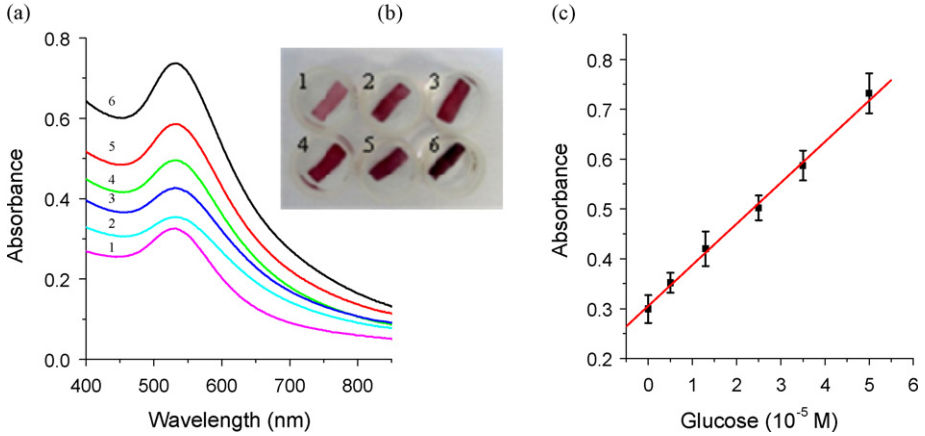

Fig. 5. (a) Absorbance spectra of the gold-functionalized CDMSs upon reaction with 1×10^{-4} M $HAuCl_4$, 12 μg mL^{-1} GOx in 0.02 M phosphate buffer that includes β-D(+) glucose of different concentrations: (1) 0 M, (2) 5×10^{-6} M, (3) 1.3×10^{-5} M, (4) 2.5×10^{-5} M, (5) 3.5×10^{-5} M, (6) 5×10^{-5} M. (b) Digital image showing the visible differences in color of substrates corresponding to the spectra (indicated by 1, 2, 3, 4, 5, 6). For all experiments the reaction time interval was 20 min, 32 ± 1 °C. (c) Calibration curve corresponding to the absorbance at $\lambda = 530$ nm of the gold-functionalized CDMSs upon analyzing β-D (+) glucose of variable concentrations (experimental conditions as in Fig. 5a). Error bars are the standards of three replicates.

reaction solution. This can be ascribed to our large amount of gold seeds which act as parent ones to associate small flakes and the aged chloroauric acid in PBS optimizes the reaction conditions.

3.4. Biosensing for glucose

All the results clearly show that the optical absorbance of our sensor is sensitive to the H_2O_2-mediated enlargement of GNPs. Encouraged by these results, we applied our biosensor for the optical detection of glucose using and O_2/GOx/glucose as the H_2O_2 generating system. To obtain the calibration curve, a series of different concentrations of glucose were detected. Fig. 5a shows the spectral changes of the resulting modified substrates in the presence of variable concentrations of glucose. In terms of the plasmon resonance band of GNPs, we can also see a visible enhancement in intensity. Similar to H_2O_2, the modified substrates are also shown to undergo visible color changes after reaction with variable concentrations of glucose in $HAuCl_4$/GOx/O_2 system. Fig. 5b represents their digital photograph in which the color changes gradually from rose pink to mulberry. Furthermore, the peak position of the optical absorbance of gold simultaneously also undergoes a red shift of ~12 nm, which can be attributed to the H_2O_2-mediated enlargement of GNPs. The calibration curve corresponding to the optical detection of glucose is presented in Fig. 5c which is derived from the intensity change of the LSPR peaks of the GNPs. The linear response range of our functionalized substrates to glucose concentration was from 5×10^{-6} to 5×10^{-5} M with a linear equation of Abs = 0.30517 + 0.08238 c (10^{-5} M) (R = 0.99807, n = 6). However, the response amplitude of spectral intensity from ~0.30 to ~0.73 was great higher than that from ~0.17 to ~0.29 with glucose concentration from 5×10^{-6} to 3×10^{-4} M on glass supports (Zayats et al., 2005). This result and phenomena is similar to H_2O_2, and consists with our expectations. The TEM measurements further support the enlargement of the GNPs on the surface of CDMSs. Fig. S1a shows the TEM image of gold seeds modified to CDMS. After reaction with glucose (5×10^{-5} M) for 20 min they were enlarged to ~12 nm (Supplementary data, Fig. S1b).

4. Conclusion

We have fabricated a highly sensitive biosensor by directly incorporating GNPs onto CDMSs. The H_2O_2-mediated growth of the GNPs enabled us to develop a substrate detection system using glucose as a model analyte. A key point of this paper, which gave our sensor special properties different from other ones based on immobilized GNPs, is our choice of such a transparent lamella as substrate. Taking advantage of its great surface area, much more gold seeds were immobilized onto CDMSs. Thus the optical response was amplified and improved sensitivity was gained. In particular, the growth of GNPs on CDMSs results in a visible color change in response to variable concentration of H_2O_2 as well as glucose, which entitles our biosensor a promising candidate as a preliminary screening device. The method described here is simple, rapid, and has potential application in visual detection of qualitative or semiquantitative analysis. It may be inspiring for useful application of bio-related matrices and really broaden our view in biosensor design.

Acknowledgements

This research is supported by National 863 High-Tech Program of China (2007AA022007) and the International Cooperation Project of Ministry of Science and Technology of China (No. 2008DFA51180).

Appendix A. Supplementary data

Supplementary data associated with this article can be found, in the online version, at doi:10.1016/j.bios.2009.07.014.

References

Bandel, K., Boletzky, S.v., 1979. Veliger 21, 313–354.
Baron, R., Zayats, M., Willner, I., 2005. Anal. Chem. 77, 1566–1571.
Bassi, R., Prasher, S.O., Simpson, B.K., 2000. Sep. Sci. Technol. 35, 547–560.
Birchall, J.D., Thomas, N.L., 1983. J. Mater. Sci. 18, 2081–2086.
Chen, H.H., Suzuki, H., Sato, O., Gu, Z.Z., 2005. Appl. Phys. A 81, 1127–1130.
Ding, S.H., Qian, W.P., Tan, Y., Wang, Y., 2006. Langmuir 22, 7105–7108.
Domard, A., 1987. Int. J. Biol. Macromol. 9, 98–104.
Grabar, K.C., Freeman, R.G., Hommer, M.B., Natan, M.J., 1995. Anal. Chem. 67, 735–743.
Gu, Z.Z., Horie, R., Kubo, S., Yamada, Y., Fujishima, A., Sato, O., 2002. Angew. Chem. Int. Ed. 41, 1153–1156.
Jia, X.P., Ma, X.Y., Wei, D.W., Dong, J., Qian, W.P., 2008. Coll. Surf. A: Physicochem. Eng. Asp. 330, 234–240.
Jia, X.P., Qian, W.P., 2008. J. Nanosci. Nanotechnol. 8, 4370–4376.
Jia, X.P., Qian, W.P., Wu, D.J., Wei, D.W., Xu, G.L., Liu, X.J., 2009. Coll. Surf. B: Biointerf. 68, 231–237.
Ma, Z.F., Sui, S.F., 2002. Angew. Chem. Int. Ed. 41, 2176–2179.
Nath, N., Chilkoti, A., 2002. Anal. Chem. 74, 504–509.
Ogasawara, W., Shenton, W., Davis, S.A., Mann, S., 2000. Chem. Mater. 12, 2835–2837.
Schmitt, J., Machtle, P., Eck, D., Mohwald, H., Helm, C.A., 1999. Langmuir 15, 3256–3266.
Shen, G.Y., Wang, H., Shen, G.L., Yu, R.Q., 2007. Anal. Biochem. 365, 1–6.
Shlyahovsky, B., Katz, E., Xiao, Y., Pavlov, V., Willner, I., 2005. Small 1, 213–216.
Tan, Y., Qian, W.P., Ding, S.H., Wang, Y., 2006. Chem. Mater 18, 3385–3389.
Wang, J.L., Wang, F., Zou, X.Q., Xu, Z.A., Dong, S.J., 2007a. Electrochem. Commun. 9, 343–347.
Wang, Y., Qian, W.P., Tan, Y., Ding, S.H., Zhang, H.Q., 2007b. Talanta 72, 1134–1140.
Wang, Z.Y., Liu, S., Wu, P., Cai, C.X., 2009. Anal. Chem. 81, 1638–1645.
Xue, M.H., Xu, Q., Zhou, M., Zhu, J.J., 2006. Electrochem. Commun. 8, 1468–1474.
Yang, J., Yang, T., Feng, Y.Y., 2007. Anal. Biochem. 365, 24–30.
Yan, W., Feng, X.M., Chen, X.J., Hou, W.H., Zhu, J.J., 2008. Biosens. Bioelectron. 23, 925–931.
Yu, A.M., Liang, Z.J., Cho, J., Caruso, F., 2003. Nano Lett. 3, 1203–1207.
Zayats, M., Baron, R., Popov, I., Willner, I., 2005. Nano Lett. 5, 21–25.
Zhang, S.B., Wu, Z.S., Guo, M.M., Shen, G.L., Yu, R.Q., 2007. Talanta 71, 1530–1535.
Zhang, S.X., Wang, N., Yu, H.J., Niu, Y.M., Sun, C.Q., 2005. Bioelectrochemistry 67, 5–22.
Zhou, N., Wang, J., Chen, T., Yu, Z.G., Li, G.X., 2006. Anal. Chem. 78, 5227–5230.